Accepted Manuscript

Research papers

Soil-water content characterisation in a *modified Jarvis-Stewart* model: a case study of a conifer forest on a shallow unconfined aquifer

Adrien Guyot, Junliang Fan, Kasper T. Oestergaard, Rhys Whitley, Badin Gibbes, Margaux Arsac, David A. Lockington

Please cite this article as: Guyot, A., Fan, J., Oestergaard, K.T., Whitley, R., Gibbes, B., Arsac, M., Lockington, D.A., Soil-water content characterisation in a *modified Jarvis-Stewart* model: a case study of a conifer forest on a shallow unconfined aquifer, *Journal of Hydrology* (2016), doi: http://dx.doi.org/10.1016/j.jhydrol.2016.11.041

Soil-water content characterisation in a *modified Jarvis-Stewart* model: a case study of a conifer forest on a shallow unconfined aquifer

Adrien Guyot[a,b,*], Junliang Fan[a,c], Kasper T. Oestergaard[a], Rhys Whitley[d], Badin Gibbes[a], Margaux Arsac[a], David A. Lockington[a,b]

[a] School of Civil Engineering, The University of Queensland, Brisbane 4072, Australia

[b] National Centre for Groundwater Research and Training, Adelaide 5001, Australia

[c] College of Water Resources and Architectural Engineering, Northwest A&F University, Yangling 712100, China

[d] Department of Biology, Macquarie University, North Ryde Sydney 2109, Australia

* Corresponding author: a.guyot@uq.edu.au. Advanced Engineering Building, School of Civil Engineering, The University of Queensland, St. Lucia 4072, Australia

Abstract

Groundwater-vegetation-atmosphere fluxes were monitored for a subtropical coastal conifer forest in South-East Queensland, Australia. Observations were used to quantify seasonal changes in transpiration rates with respect to temporal fluctuations of the local water table depth. The applicability of a *Modified Jarvis-Stewart* transpiration model (MJS), which requires soil-water content data, was assessed for this system. The influence of single depth values compared to use of vertically averaged soil-water content data on MJS-modelled transpiration was assessed over both a wet and a dry season, where the water table depth varied from the surface to a depth of 1.4 m below the surface.

Data for tree transpiration rates relative to water table depth showed that trees transpire when the water table was above a threshold depth of 0.8 m below the ground surface (water availability is non-limiting). When the water table reached the ground surface (i.e., surface flooding) transpiration was found to be limited. When the water table is below this threshold depth, a linear relationship between water table depth and the transpiration rate was observed. MJS modelling results show that the influence of different choices for soil-water content on transpiration predictions was insignificant in the wet season. However, during the dry season, inclusion of deeper soil-water content data improved the model performance (except for days after isolated rainfall events, here a shallower soil-water representation was better). This study demonstrated that, to improve MJS simulation results, appropriate selection of soil water measurement depths based on the dynamic behaviour of soil water profiles through the root zone was required in a shallow unconfined aquifer system.

Keywords

2

1. Introduction

Tree transpiration is a significant component of the hydrological cycle in forest systems and as such its quantification and forecasting is important for the development of robust, defensible and sustainable water management strategies (Schlesinger and Jasechko, 2014). The four environmental variables that are the primary drivers of transpiration are solar radiation, vapour pressure deficit, soil moisture and leaf area index (Jarvis, 1976; Harris et al, 2004; Asbjornsen et al., 2011; Whitley et al., 2013). Transpiration can be modelled using either physical or empirical analyses of these variables. Potential evapotranspiration is often calculated by the physically-based Penman-Monteith (PM) equation (1965). Building on the PM equation, Jarvis (1976) and later Stewart (1988) further describe the stomatal (or canopy) conductance using an empirical approach, which are usually named as a *Jarvis-* or *Jarvis-Stewart*-type model (see Table 1). This approach allows an estimate of canopy water flux for a site under specific meteorological conditions using the PM equation, without requiring field data of canopy conductance. Recently, empirical approaches were developed to quantify transpiration directly, circumventing the need for canopy conductance data (Whitley et al., 2008, 2009, 2013), and this approach is termed the "modified *Jarvis-Stewart* model".

< Table 1 here please >

All of these empirical models assume that soil-water content is a key variable for accurate simulation of transpiration (see Table 1; Granier and Lousteau (1994), Harris et al. (2004), Liu et al. (2009) etc.). In practice, the calibration of the soil-water content function used in the models uses either soil-water content observations at different time intervals and depths, or empirical relationships between soil types and soil-water availability (Table 1). In earlier studies, the time interval between manual measurements of the soil moisture varied from days (Stewart 1998), to a week (Harris et al. 1994) to 10 days (Granier and Lousteau 1994, Liu et al. 2009). More recently, higher-frequency measurements of 15 minute intervals (Garcia-Santos et al. 2009, Whitley et al. 2013) have allowed researchers to describe changes in the soil-water content directly after a rainfall event. While some researchers integrate the soil-water content over the entire vertical soil profile (Stewart 1988, Harris et al. 2004, or Liu et al. 2009), others consider the soil water content solely at a specific depth (Whitley, 2008; 2009). There is, therefore, no clear convergence towards a standard approach for characterising soil-water content.

Another aspect of these empirical models is that they do not account for diurnal variation (*i.e.* night-time transpiration). Night-time water use by trees was initially assumed negligible (Daley and Phillips, 2006), but recent advances in sap flow and stem diameter variation measurement techniques have demonstrated that night-time transpiration occurs in multiple ecosystem types (Dawson et al., 2007, Zeppel et al., 2010; 2013). Existing literature indicates that night-time water use is far from negligible, and can account for up to 30% of daily water use in some ecosystems (Daley and Phillips, 2006, Dawson et al., 2007, Novick et al., 2009).

Like other shallow aquifer areas around the world, commercial conifer forests have replaced large areas of native forests for timber production in subtropical coastal Australia. This region in Australia is characterized by pronounced wet and dry seasons, sandy soils and shallow unconfined aquifers (*i.e.* shallow water table conditions when water table at depth < 2m from the ground surface). Under these shallow groundwater conditions, the vertical extent of the root zone in conifer forests can be limited as a response to frequent waterlogging. Also, variations in the water table depth may result in seasonal changes in the access to soil water by forests. Soil-water availability is typically assumed to be unlimited in these environments and evapotranspiration is often assumed to be equivalent to the potential evapotranspiration rate estimated by the PM equation combined with a crop factor. The crop factor or crop coefficient is usually defined as the ratio of the observed evapotranspiration for the studied crop over the potential evapotranspiration at the same location (Allen et al., 1998). However, even if that assumption is a useful and conservative estimate, given the dynamic hydrology of shallow sandy aquifers, this approach may lead to an overestimate of the actual evapotranspiration and thus transpiration. For permeable soils, the vertical distribution of soil-water content varies significantly within the root zone over daily timescales. Here, a single measurement of the soil-water content at a given depth can provide limited information, and may lower the accuracy of transpiration estimates compared to multiple depth and/or optimal depth soil-water content observations, especially in the context of seasonal rainfall events.

The current study thus aimed to quantify seasonal changes in transpiration rates with fluctuating water table depth for a subtropical coastal conifer forest in South-East Queensland, Australia. The applicability of

4

the *Modified Jarvis-Stewart* transpiration model to this shallow aquifer system was assessed. The specific objectives of the study were:

(i) to acquire field observations of groundwater-soil-water-vegetation-atmosphere interactions over both a wet and a dry season for a representative plot within the conifer forest;

(ii) to establish relationships between the transpiration rate and the abiotic drivers of transpiration, with a particular focus on seasonal variability of transpiration with fluctuations of soil-water content and water table depths; and

(iii) to investigate the effect of choice of depth of soil-water content on transpiration estimates, compared to the use of vertically averaged values in a MJS model.

In addition, the effect of night-time transpiration on the overall transpiration rate was quantified and discussed.

2. Material and Methods

2.1 Site description

< Figure 1 here please >

Figure 1 shows the location of the study site within a pine plantation located on Bribie Island (26°59′2.534″S, 153°08′16.857″E) on the East coast of Australia. Bribie Island is a sand barrier island near Brisbane and has an average width of 5 km with a total area of 144 km^2 (Isaacs and Walkers, 1983). This Island has a low relief with an average elevation of 5 m above Australian Height Datum (AHD), or roughly Mean Sea Level. The region has a humid subtropical climate (Köppen climate classification Cfa) with a distinct warm wet summer (November to April) and a mild dry winter (May to September). The average annual rainfall is approximately 1605 ± 279 mm, with 77 % of annual rainfall occurring in the wet season based on data from 1970 - 2010 (Bureau of Meteorology, station 040842). The mean maximum air temperature is 29.0 °C in January with an average relative humidity of 64 %, and the mean minimum air temperature is 20 °C in July with a corresponding average air relative humidity of 59 %. Over the 2010-2015 period daily pan evaporation varied from 2.8 mm day^{-1} (June) to 7.3 mm day^{-1} (October – January) (Brisbane Airport Bureau of Meteorology Station (station 040842)). The mean annual pan evaporation values recorded at the same station were 1650 mm year^{-1} over the 2008-2011 period.

Our study was conducted over a 13 month period from January 2012 to January 2013 during which an extended wet season (January to July 2012) occurred (Figure 2a).

< Figure 2 here please >

This wet period was then followed by dry conditions lasting from August 2012 to January 2013. During the study period, rain was observed on 135 days out of 386 days. Of these 135 days, a daily rainfall between 2 and 10 mm day^{-1} was observed on 89 days, and rainfall in excess of 10 mm day^{-1} occurred on 42 days. (Figure 2a). The pine plantation at the site was established in 2001 and comprises hybrid pines (*Pinus elliottii Engelm var. elliottii x Pinus caribaea Morelet var. hondurensis*) with a stand density of 840 trees per hectare, a mean diameter at breast height (1.3 m) of 0.223 ± 0.032 m, and a mean tree height at the time of the study of 13 ± 0.5 m. The understory consists of a sparse covering of ferns. An unconfined aquifer lying over

cemented low permeability layers is considered extensive throughout the island and consists of unconsolidated fine to medium sand (Hodgkinson et al., 2008; Fan et al., 2014).

Plantation managers regularly clear the understory throughout the year. As a result, the understory predominantly consists of very shallow-rooted occasional ferns and no grass or weeds. Although pine needles create a thin surface layer, the topsoil had very low organic matter content. Theoretically, water stored in the pine needle litter layer could be used by the trees during transpiration, however, because it was so thin, we hypothesised that the water occurring within that surface layer could be neglected as a source of water for the tree transpiration. This hypothesis was supported by visual observations, notably the absence of superficial roots within the litter layer.

2.2 Transpiration observations

Sap flux density (SFD, cm^3 cm^{-2} d^{-1}) was measured using commercially available sap flow sensors based on the heat ratio method (HRM) (ICT International Pty Ltd, Armidale, Australia). The HRM is an improvement of the compensation heat pulse method (Burgess et al., 2001) which allows low and reverse rates of sap flow in xylem tissue to be measured. A total of 6 trees were instrumented with HRM at breast height within a 50 m x 50 m plot (comprising a total of 210 trees) with two HRM sensors per tree (*i.e.* North and South cardinal direction) (Figure 1). Each sensor had 2 measurement-point located at 12.5 mm and 27.5 mm into the sapwood. A previous study on the same species (Guyot et al., 2015) showed that this setup, combining 2 sensors with 2 measurement-point at different depth provided reasonable accuracy as compared to a benchmark of 24 measurement points per tree. Sap flow measurements were corrected for wounding effects following Burgess et al. (2001) based on the wound width determined from dummy probes installed simultaneously with SFD measurements. Wound width was determined from colour distinction and was measured from digital images (Olympus μ 770 *SW* digital camera) taken after one month, six months and twelve months using ImageJ 1.47v software (National Institutes of Health, USA). The average wound width was 2.5 ± 0.3 mm and did not seem to increase over the study period after its initial stabilisation (*i.e.* one month). Therefore, it was assumed that the wound width was constant over the study period and between trees, although small variations between dummy probes were observed. Measurements of gravimetric sapwood moisture content were conducted during wet conditions (*i.e.* February 2012) and during the

7

transition to dry conditions (*i.e.* November 2012). Each time a total of 10 samples were collected. Gravimetric sapwood moisture content was found not to vary significantly between dry and wet conditions with an average value of 0.98 ± 0.18 kg$_{water}$ kg$_{dry-wood}^{-1}$. A constant value of 0.98 kg$_{water}$ kg$_{dry-wood}^{-1}$ was used with a dry wood density of 520 ± 8 kg m^{-3} for correction following Vandegehuchte & Steppe (2012c). Furthermore, each measurement probe was corrected for offset (*i.e.* probe misalignment) by examining the SFD at night when VPD and wind speed were approximately null. Zeppel et al. (2010) found no significant difference in offset corrections using this method compared to cutting the sapwood below and above the measurement probes.

First, SFD measurements were scaled up to single-tree transpiration fluxes, T_{TREE} (mm h^{-1}) using a relationship between the tree diameter at breast height DBH (m) and the sapwood area $A_{sapwood}$ (mm^2). This relationship was established based on a sample of 11 trees (with DBH ranging from 17.3 cm to 22 cm and sapwood areas ranging from 114 cm^2 to 163 cm^2) that were cut after the experiment and following Cermak and Nadezhdina (1998). Digital images were analysed with ImageJ 1.47v (National Institutes of Health, USA) to determine the sapwood areas which was clearly identified by a distinct clear colour as compared to the darker heartwood (Guyot et al., 2013) and lead to Eq. (2) (with $R^2 = 0.92$):

$$A_{sapwood} = \sum_{i=1}^{n} 0.04 \, DBH_i + 106 \tag{2}$$

Forest transpiration (T_{STAND}, mm day^{-1}) was then calculated from the average of the single-tree transpiration (T_{TREE}) from the six trees, and multiplied by the stand density (210 trees per plot, equivalent to 840 trees per ha) following Cermak and Nadezhdina (1998). We also evaluated the uncertainty associated with the spatial variability of T_{STAND} by calculating the standard deviation of T_{STAND} for the individual transpiration estimates for 6 trees (T_{TREE}) (plotted on Figure 2d).

2.3 Micrometeorology

Data on rainfall intensity and duration were collected by a tipping bucket rain gauge (RIMCO 7499, McVan Instruments, Mulgrave, VIC, Australia) at the local water management agency's (SEQwater) automatic

weather station located 2.5 km from the study site. Measurements of air temperature (T_a, °C) and relative humidity (RH, %) (HMP155 sensor, Vaisala, Finland), wind speed (u_2, m s^{-1}) and direction (° magnetic) (03002 wind sentry set, RM Young, USA) and net radiation (R_n, W m^{-2}) (CNR4 net radiometer, Kipp & Zonen, Delft, The Netherlands) were conducted at 2 m above the plantation forest canopy on a 15 m mast located in the centre of the study site. These meteorological variables were measured at a frequency of 1-min and averaged over 15-min intervals then recorded with a data logger (CR3000, Campbell Scientific, USA). Vapour pressure deficit (VPD, Pa) was inferred from T_a and RH following Goldstein et al. (1998). Penman's (1948) potential evapotranspiration as given in Shuttleworth (1993) and Donohue et al. (2010) was computed using the daily-observed atmospheric variables, *i.e.* RH, R_n, u_2 and T_a following equation (1):

$$\mathbf{PET} = \mathbf{PET}_R + \mathbf{PET}_A = \frac{\Delta}{\Delta + \gamma} R_n + \frac{\gamma}{\Delta + \gamma} \frac{\mathbf{6430(1 + 0.536}u_2\mathbf{)} \, VPD}{\lambda}$$

(1)

where, PET is the potential evapotranspiration (mm day^{-1}), PET_R and PET_A represent respectively the radiative and aerodynamic components of the Penman equation, R_n is net radiation (in equivalent mm day^{-1}), Δ is saturation slope vapour pressure curve at T_a (kPa °C^{-1}), γ is the psychrometric constant (kPa °C^{-1}) and λ is the latent heat of vaporisation of water (2.45 10^6 J kg^{-1}).

In order to assess the "performance" of the tree stand estimates of transpiration for a given atmospheric condition, we defined "transpiration efficiency" which equals to the ratio of observed stand transpiration to the potential evapotranspiration (Efficiency = T_{STAND} / PET). Small values of this ratio will thus represent a combination of relatively low observed transpiration rates and very suitable conditions for transpiration (high PET). On the other hand, higher values of the ratio will correspond to high rates of observed transpiration and average or not suitable conditions for transpiration (low PET).

2.4 Leaf area index

Leaf area index (LAI) was measured three times over the course of the monitoring period in order to account for adjustments in canopy leaf area. The first measurement was conducted at the end of the summer (late February, 2012) followed by measurements in winter (late June, 2012) and at the end of spring (mid-November, 2012). Measurements of LAI were completed using digital images combined with image processing using a commercial software package (MATLAB 2012a, The Mathworks Inc., Natick, MA) developed by Fuentes el al. (2008). Images were taken with an Olympus μ 770 *SW* digital camera using automatic exposure and mounted at zenith angle on a 1.5 m levelled tripod. Five transects of 50 m with an image distance of 5 m yielded a total of 55 images. LAI was calculated following the method detailed in Fuentes et al. (2008).

2.5 Soil-water content and water table depth

Soil-water content (SWC) and soil temperature were measured using four Time Domain Reflectometers (TDR) (CS650, Campbell Scientific, Utah) installed at depths of 0.2 m, 0.4 m, 0.6 m and 0.8 m below ground surface. The sensors were connected to a data logger (CR3000, Campbell Scientific, Utah) setup to record data 15 minute intervals. Due to microtopographic variations at the site (up to 0.1 m), the shallowest measurements were taken at a depth of 0.2 m, and this was selected as the starting depth. As a result of relatively high water table elevations during the dry season of 2012, installing sensors deeper than 0.8 m from the soil surface (below the water table at that time) was not possible due to slumping of the fine sand. Lateral variability of the soil-water content within the plot is considered to be relatively limited based on observations of the particle size distribution for soil samples taken at 4 depths from 2 different pits approximately 50 m apart.

Soil samples showed the soil profile to be characterised by a fine sand that was uniform across all depths. Bulk density was measured every 20 cm at depth from the surface, and very little variation with depth was observed ($\rho_{bulk} = 1.5 \pm 0.03$ g/cm^3). Site-specific calibration of the TDRs was completed following Western et al. (2002) using a constant bulk density of 1.5 g/cm^3 also including correction from temperature effects. We encountered technical issues leading to gaps in the SWC observations towards the end of 2012 It was decided not to use interpolation methods for these gaps because of the occurrence of small rainfall events

10

during that time that might have increased SWC, thus these short periods were not considered in further analysis.

Water table depth (relative to ground surface) was measured at 15-min intervals in a 2.5 m deep well located at the centre of the site using a vented pressure transducer (Level Troll 500, In-Situ Inc., USA)for the durations of the study period. Manual water level measurements were conducted on a regular basis using a dip meter, and validated the pressure transducer measurements with an accuracy of 0.5 cm.

2.6 Modified Jarvis-Stewart model

The MJS model was calibrated by fitting seven parameters to our observations of transpiration derived from sap flux density measurements, and was used to make predictions of transpiration (T_{MJS}, mm h^{-1}) at this site. Similarly to previous studies (Whitley et al., 2013), we assumed that the canopy was well coupled to the atmosphere. The expression for modelled transpiration is given by (Eq. 4):

$$T_{MJS} = T_{MJS\,max} f_1(R_n) f_2(VPD) f_3(SWC) \tag{4}$$

where $T_{MJS\,max}$ is the maximum transpiration (mm h^{-1}) that is proportionally modified by three functional relationships, $f_{1..3}$. These functional relationships represent the independent responses of transpiration to net radiation $f_1(R_n)$ (Eq. 5), vapour pressure deficit $f_2(VPD)$ (Eq. 6), and soil moisture or soil-water content $f_3(SWC)$ (Eq. 7). The expression for $f_1(R_n)$ relationship is given by (Eq. 5):

$$f_1(R_n) = \frac{R_n}{R_n + k_r} \tag{5}$$

where, R_n is net radiation (W m^{-2}) and k_r was a fitted parameter. The expression for the $f_2(VPD)$ relationship is given by (Eq. 6):

11

$$f_2(VPD) = e^{\left[-\frac{k_{d1}}{(VPD+k_{d2})}(VPD-VPD_{max})^2\right]}$$
(6)

where, VPD is the vapour pressure deficit (kPa), VPD_{max} (kPa) was the maximum recorded hourly VPD, and k_{d1} (-) and k_{d2} (-) were fitted parameters.

Modifications have been made to the f_3(SWC) published in Whitley et al. (2013). A sigmoidal function has been implemented to achieve better model convergence. The expression for the f_3(SWC) relationship is given by (Eq. 7):

$$f_3(SWC) = \frac{1+e^{(k_s SWC)}}{1+e^{-k_s(SWC-SWC_w)}}$$
(7)

where, SWC is the measured volumetric soil-water content (cm^3 cm^{-3}), SWC_w was the site-specific soil-water content wilting point parameter, and k_s (-) was a parameter describing the rate of change in transpiration as soil-water content declines. This new function is functionally equivalent to previous piece-wise linear expressions, but avoids autocorrelation between $T_{MJS\,max}$ and the SWC critical point. Both SWC_w and k_s were fitted parameters.

2.7 Model evaluation

The model was fitted to an ensemble of hourly data (Table 2, Nb. Days = 60, N = 720 data-points) consisting of observed transpiration and local meteorology that were representative of both wet and dry seasons at the study site (excluding night-time values). The calibration dataset consisted of 20 days from the wet period (February to March 2012), 20 days from a transition period (August to September 2012) and 20 days from the dry season (December 2012 to January 2013). Validation was then performed on the complete set

12

of hourly data, excluding the 60-day dataset used for calibration (Table 3, Nb. Days varying from Nb. Days = 264 for SC20 to Nb. Days = 194 for SC80, *i.e.* N = 3165 data-points for SC20 and N = 2323 data-points for SC80). This partition between calibration and validation was a trade-off between enough calibration/training data and sufficient validation and testing data. The statistical software package R (http://www.r-project.ord/) was used to calibrate and validate the model. The model optimization to the dataset was conducted using the *GENetic Optimization Using Derivatives* algorithm (Mebane and Sekhon, 2011) by minimising the weighted sum of the square of the errors (WSSE) (Eq. 8).

$$\textbf{WSSE} = \sum_{i=1}^{N} \left(\frac{Obs_i - Mod_i}{\sigma_i} \right) \tag{8}$$

where, Obs_i was the observed stand transpiration, Mod_i was the predicted stand transpiration determined from the input variables and model parameters, N was the number of observations and σ was the error on measurements (here the standard deviation from the average of the 12 measurement points was used as an approximation of σ).

To evaluate the model performance, the root mean square error (RMSE) and coefficient of determination (R^2) were selected. RMSE was selected to measure how much the model prediction deviates from the observed data and R^2 was used to explore linearity between the observations and the outputs of the model.

2.8 Modelling scenarios

A total of five modelling scenarios were implemented in this study to investigate the influence that SWC at depth has on the transpiration values generated by the MJS model. The labels SC20, SC40, SC60 and SC80 represent scenarios where individual SWC measurements occurred at depths of 0.2, 0.4, 0.6 and 0.8 m from the soil surface and were used as the input for volumetric soil-water content in the MJS model. The SC-Int. label represents the integrated SWC over a depth range of 0.2 m to 0.8 m using the same weighting per depth interval in the averaging of SWC.

3. Results

3.1 Abiotic drivers, soil-water content and water table

Observed transpiration T_{STAND} from January 2012 to January 2013 captured a distinct wet and dry season (Figure 2). The annual rainfall for 2012 was 1902 mm and the annual observed transpiration 984 mm. During this study, the highest rainfall observed was 238 mm day^{-1}, while the highest level of transpiration was 4.8 mm day^{-1}. The lowest recorded daily transpiration was 0.1 mm day^{-1}, which occurred during a rainy day.

The first part of the year (January to July 2012) saw saturated conditions at depths 0.4, 0.6 and 0.8 m below the surface with a constant SWC of 0.28 cm^3 cm^{-3} for that period. The shallowest observation of SWC at 0.2 m depth fluctuates during that first part of the year, with relatively dry conditions in January (around 0.1 cm^3 cm^{-3}), peaking at 0.40 cm^3 cm^{-3} shortly after the first rainfall events and fluctuating around 0.28 cm^3 cm^{-3} until July 2012. We measured smaller dry bulk density values (1.43 ± 0.02 g cm^{-3}) at 0.0 to 0.2 m depth as compared to dry bulk densities of 1.57 ± 0.09 g cm^{-3} at 0.2 to 0.8 m depths, which supports higher values of SWC at saturation (up to 0.4 cm^3 cm^{-3}) near the surface. Soil-water content varied from saturated conditions across the vertical profile (high water table) to very dry when the water table was at its lowest (*i.e.* 1.4 m below ground surface). During the dry stage, SWC was less than 0.02 cm^3 cm^{-3} at depths of 0.2 m to 0.4 m and declining from 0.2 to 0.1 cm^3 cm^{-3} at a 0.8 m depth (Figure 2e).

The average maximum hourly R_n ranged from 1000 W m^{-2} in the summer to 700 W m^{-2} in winter. The average maximum recorded VPD in an hour ranged from 4.8 kPa in summer to 2.3 kPa in winter.

< Figure 3 here please >

Figure 3a and 3b show T_{STAND} *versus* R_n and VPD for the different seasons. Under wet summer and autumn 2012, T_{STAND} plateau to around 0.4 mm h^{-1} as R_n and VPD increases. During the dry summer of 2013, recorded transpiration reached a plateau at a considerably lower T_{STAND} (at 0.2 mm h^{-1}) compared to the wet summer of 2012.

14

LAI measurements showed little variation over the seasons, with a value of 2.1 ± 0.6 in the summer (February, 2012) reducing to 1.8 ± 0.3 in the winter (July, 2012) and increasing slightly to 1.9 ± 0.4 in spring (November, 2012).

< Figure 4 here please >

Figure 4 shows the relationship between T_{STAND} and PET ratio which represents the transpiration efficiency versus the water table depth. Higher values of the ratio represent an unlimited access to soil-water, whereas lower values correspond to a limited or non-existent access to the soil-water. A linear regression is also shown for the values of the ratio below a threshold depth of 0.8 m. The 0.8 m depth was chosen based on the observed shift and decrease in the T_{STAND} and PET ratio below that depth.

3.2 Model calibration and validation

< Table 2 here please >

A total of seven parameters were determined for each SWC at depth scenario (Table 2). $T_{MJS\,max}$ is slightly under the maximum recorded T_{STAND} at the site (*i.e.* 0.4 mm h^{-1}), except for the SC80 scenario, where $T_{MJS\,max}$ is large compared to the other scenario values (*i.e.* 0.70 mm h^{-1}). All fitted parameters representing R_n and VPD are similar, which is expected, as by definition the atmospheric conditions are the same for all scenarios. On the other hand, the soil-water content parameters (SWC_w and k_s) were spread over a much wider range. For example, k_s, which represents the rate of change of transpiration as soil water declines, is a factor of 10 larger for SC20 as compared to the deeper SC60 and SC80. Similarly, the SWC_w (*i.e.* the specific wilting point) is a factor of 10 larger for SC80 as compared to the surface SC20 and SC40. The relatively large standard errors on kd_1, kd_2 and SWC_w could suggest that the model is over-parameterized (*i.e.* more parameters than can be estimated from the data).

The functional boundaries for R_n and VPD (Eq. 5 and Eq. 6) capture the variations found in the observations (Figure 3) with exceptions during the wetter periods. Function boundaries for $f_1(R_n)$ and f_2(VPD) are only shown for the SC20, as each scenario show similar trends.

< Figure 5 here please >

In figure 5, one can see that the soil-water content function boundaries capture the majority of data points, except for SC80 (Figure 5d). Data points for SC80 outside the function boundaries do not seem to be consistent with any particular season. The overall performance of the simulations for the fitted parameters, when applied to the validation period, showed RMSE ranging between 0.036 and 0.064 (Table 3) with a consistent linear relationships between observed and predicted values for all scenarios (Table 3).

< Figure 6 here please >

< Table 3 here please >

The model performance for the validation dataset using the calibrated parameters resulted in RMSE values ranging from 0.036 to 0.064 (Table 3, Figure 6) and indicates a strong linear relationship between observed and predicted values (slopes of the linear regressions ranging from 0.95 to 1.02). For SC60 and SC80 (Figure 6 (c) and (d)), 92 and 91 % of variance were explained respectively, which is in the same range found in other applications of the model (Whitley et al., 2008; 2009).

4. Discussion

4.1 Forest transpiration and water table elevation

While the first part of the study period was characterised by saturated soil-water conditions with a high water table, the second part of the period (with drier conditions) included more dynamic conditions with variations in T_{STAND} related to soil-water availability. The sharp reduction in T_{STAND} during December 2012 and January 2013 suggests a shallow root zone with a distinct gradient in root density. Visual trench inspections made when installing soil sensors revealed a high density of roots in the upper 0.5 m of the soil profile gradually reducing to a few roots around 1 m depth from the surface. In Figure 4, the T_{STAND}/PET ratio is relatively stable (between 0.30 and 0.45) when the water table is between -0.2 m and -0.8 m and only falls below 0.30 when the soil is saturated (water table elevation above -0.2 m, *i.e.* at, or above the ground surface which happens during autumn and winter of 2012). This indicates that the trees have unlimited access to the soil-water while the water table elevation is above -0.8 m, except when the water table reaches the surface such that there is flooding, in which case transpiration is limited. This is thought to

16

occur because flooding causes oxygen deprivation in the tree root systems (Kreuzwieser et al. 2004). When the water table drops below -0.8 m, the decrease in T_{STAND}/PET ratio suggests that the actual transpiration did not reach its maximum based on the atmospheric conditions, likely due to limited access to soil-water. When the water table falls further, the T_{STAND}/PET ratio follows a linear decrease (a linear regression for spring of 2012 and summer of 2013 is shown in Figure 4) with increasing depth to water table and a ratio close to zero when the water table is at -1.4 m (summer of 2013). This linear decrease of T_{STAND}/PET ratio with depth could mean that the root zone density/distribution decreases linearly with depth, or that the soil-water content above the water table increases linearly with height above the water table, or both. Trees can store water in the roots and in the stem through redistribution (Burgess at al., 1998), which could provide water supply for persistent transpiration despite no access to the water table by the root system, thus creating inertia between water table drop and a reduction of transpiration. For this shallow aquifer environment, where the root density is concentrated close to the surface, the water table depth is thus controlling the available soil-water content (through a direct access of the roots to the water table or through the available soil-water above the water table) and thus transpiration. When soil moisture drops below a critical threshold, trees appear to reduce their stomatal conductance to prevent xylem cavitation as Oren et al. (1998) have shown for *Pinus taeda* (for volumetric moisture content below 0.22 in their case).

4.2 Representation of the soil-water content in MJS

Fitted soil parameters for each scenario (Table 2) show differences which are reflected in the mean bias error for the cumulative T_{STAND} and T_{MJS} (Table 3). Differences occur during the dry season when the deeper scenarios (*e.g.* SC60 and SC80) cannot capture the increase in T_{STAND} because of small rainfall events for which the short-time response would not be recorded at these depths (60 cm and 80 cm). For these small rainfall events (*e.g.* less than 10 mm), SC20 was found to best capture the increase in T_{STAND}, while SC60, SC80 and SC-Int. were incapable of simulating T_{STAND} accurately. This is somewhat expected for SC-Int. due to small changes the overall water content of the soil profile. This result suggests that the use of SWC input from deeper depth will result in an under prediction of transpiration during dry conditions when small rainfall events occur. An alternative to the integration of SWC to compute our SC-int. could consider greater

17

weighting in the averaging of SWC for the soil zones with high root densities, but that would also increase the model complexity and site-specificity, thus reducing model usability.

The current soil moisture function of the MJS indirectly incorporates plant stress, but this is solely dependent on the calibration dataset. This constraint is needs to be considered when using this model to predict transpiration on longer time scales (*e.g.* years). Forests could be affected by stress as a result of prolonged wet or dry conditions (*e.g.* embolism, dormancy) or health issues (*e.g.* disease or insect attack) and these aspects that will be not represented by this approach. If long-term dataset are available, alternative soil moisture functions that take this into account do exist (Yang et al., 2012).

4.3 Night-time transpiration

Night-time transpiration represents a significant part of diurnal tree water use in forests (Burgess et al., 1998; Dawson et al., 2007; Zeppel et al., 2010). The night-time transpiration is not included in the evaluation of the model, as the model eliminates transpiration during night-time hours when net radiation tends to zero. For this study, the observations suggest that night-time periods account for approximately 20 % of the daily transpiration, which is significant and in the order of magnitude of other studies (Zeppel et al., 2010). A key consideration here is whether the measured night-time flux is indeed a result of transpiration or a hydraulic re-saturation of the tree stem and branches. The use of multiple evenly distributed measurement points of water movement within a tree similar to the setups found in Zeppel et al. (2010) and Pfautsch et al. (2013) could give more information on the tree water use behaviour during night-time thus enabling a partitioning of re-saturation and night-time transpiration. The MJS model could potentially benefit from the work by Wallace and McJannet (2010), where a relationship between night-time water use and a combination of VPD and soil-water content was demonstrated. Overall, the MJS model performance for this study was comparable to previous studies, with daylight differences between simulated and observed transpiration for the study period ranging from 1.7 % to 4.1 % for cumulative annual transpiration. However, if night-time water use is included, the difference between simulated and observed transpiration increase was found to range from 12.4 % to 18.3 %.

4.4 Inter-annual variability

To achieve a robust set of fitted parameters for the MJS model, a data set representing both wet and dry season conditions was necessary. Calibrating the model to wet conditions will result in an overestimation during dry periods and calibration during dry conditions will results in underestimates during the wet periods as fitted $T_{MJS\ max}$ value will not be representative of the maximum transpiration under either scenario. The $T_{MJS\ max}$ parameter is critical, as it captures a site's optimal water-use given environmental changes such as LAI and plant growth. For daily and monthly time scales, the abiotic drivers and water availability will control transpiration in forests, but on seasonal, annual and longer time scales other factors such as forest growth and health will have to be taken into account. It is acknowledged that these factors are also likely to be partly a result of water availability over the long-term. LAI is not included in the current model, but it does control seasonal transpiration (Eamus et al., 2006). LAI was measured at the site and was not found to vary significantly during the study period. LAI is consequently not expected to have a significant influence on model performance during this study period. However, for long-term applications such factors will have to be accounted for and the fitted parameters estimated in this study may no longer be applicable. In undisturbed forests, biomass may be stable over the long-term compared to plantation forests, unless affected by natural disaster (*e.g.* fire, cyclone). In plantation forest, a rotation cycle changes the forest hydraulic characteristics significantly over a rotation scheme. Long-term monitoring is required for plantation forests to capture changes in transpiration with stand age and density.

5. Conclusion

We investigated groundwater-vegetation interactions in a shallow water table environment where the water table ranged from fully saturated conditions (water table at surface) to water table levels 1.4 m below the ground surface during the study period. Observations of transpiration and water table elevation showed that trees are transpiring at rates consistent with unlimited water access conditions when the water table was above a certain threshold elevation. When the water table dropped below this threshold elevation, a linear relationship between decreasing water table depth and transpiration was observed. These observations suggest that even in forests with shallow water tables, transpiration can be water-limited, disproving an assumption that is often made while using potential evapotranspiration models.

Study results suggest a detailed characterisation of the soil-water content across the rooting depth is necessary during the dry season for the MJS model to adequately simulate the observed transpiration. During the wet season and for close to saturated conditions, the influence of the representation of soil-water content in the model was not significant for the transpiration predictions. However, during the dry season, a shallow soil-water content representation improved the transpiration observations when isolated rainfalls occurred. Study results also highlight the role of night-time transpiration and suggest that this aspect should be the focus for research to further develop this model. Finally, combining the MJS transpiration model with an evaporation model would make it more attractive for water managers and stakeholders in the perspective of improving groundwater recharge models.

Acknowledgments

Conflict of interest

The authors declare that they have no conflicts of interest.

References

Asbjornsen, H., Goldsmith, G. R., Alvarado-Barrientos, M. S., Rebel, K., Van Osch, F. P., Rietkerk, M., ... & Dawson, T. E. (2011). Ecohydrological advances and applications in plant–water relations research: a review. *Journal of Plant Ecology*, *4*(1-2), 3-22. doi: 10.1093/jpe/rtr005.

Allen, RG, Pereira, LS, Raes, D & Smith, M 1998, *Crop evapotranspiration - Guidelines for computing crop water requirements.*

Burgess, S. S., Adams, M. A., Turner, N. C., & Ong, C. K. (1998). The redistribution of soil-water by tree root systems. *Oecologia*, *115*(3), 306-311. DOI:10.1007/s004420050521.

Condon, A. G., G. D. Farquhar, and R. A. Richards. "Genotypic variation in carbon isotope discrimination and transpiration efficiency in wheat. Leaf gas exchange and whole plant studies." *Functional Plant Biology* 17.1 (1990): 9-22.

Daley, M.J. and Phillips, N.G., 2006. Interspecific variation in nighttime transpiration and stomatal conductance in a mixed New England deciduous forest. *Tree Physiology*, *26*(4), pp.411-419.

Dawson, T. E., Burgess, S. S., Tu, K. P., Oliveira, R. S., Santiago, L. S., Fisher, J. B., ... & Ambrose, A. R. (2007). Nighttime transpiration in woody plants from contrasting ecosystems. *Tree Physiology*, *27*(4), 561-575. doi: 10.1093/treephys/27.4.561

Ding, Z., Wen, Z., Wu, R., Li, Z., Zhu, J., Li, W., & Jian, M. (2013). Surface energy balance measurements over a banana plantation in South China. *Theoretical and applied climatology*, *114*(1-2), 349-363. DOI:10.1007/s00704-013-0849-5.

Donohue, R. J., McVicar, T. R., & Roderick, M. L. (2010). Assessing the ability of potential evaporation formulations to capture the dynamics in evaporative demand within a changing climate. *Journal of Hydrology*, *386*(1), 186-197. doi:10.1016/j.jhydrol.2010.03.020

Eamus, D, Hatton, T, Cook, P & Colvin, C 2006, *Ecohydrology: vegetation function, water and resource management*, 1 edn, CSIRO Publishing.

Fan, J., Oestergaard, K. T., Guyot, A., & Lockington, D. A. (2014). Estimating groundwater recharge and evapotranspiration from water table fluctuations under three vegetation covers in a coastal sandy aquifer of subtropical Australia. *Journal of Hydrology*, vol. *519*, pp. 1120-1129. DOI:10.1016/j.jhydrol.2014.08.039.

Fuentes, S, Palmer, AR, Taylor, D, Zeppel, M, Whitley, R & Eamus, D 2008, An automated procedure or estimating the leaf area index (LAI) of woodland ecosystems using digital imagery, MATLAB programming and its application to an examination of the relationship between remotely sensed and field measurements of LAI, *Functional Plant Biology*, vol. 35, pp. 1070-9. http://dx.doi.org/10.1071/FP08045

García-Santos, G., Bruijnzeel, L. A., & Dolman, A. J. (2009). Modelling canopy conductance under wet and dry conditions in a subtropical cloud forest. *Agricultural and forest meteorology*, *149*(10), 1565-1572. doi:10.1016/j.agrformet.2009.03.008.

Goldstein G, Andrade JL, Meinzer FC, Holbrook NM, Cavelier J, Jackson P & Celis A (1998) Stem water storage and diurnal patterns of water use in tropical forest canopy trees. *Plant, Cell Environ* 21:397–406. DOI: 10.1046/j.1365-3040.1998.00273.x.

Granier, A., & Loustau, D. (1994). Measuring and modelling the transpiration of a maritime pine canopy from sap-flow data. *Agricultural and Forest Meteorology*, *71*(1), 61-81. doi:10.1016/0168-1923(94)90100-7

Guyot, A., Ostergaard, K.T., Fan, J., Santini, N.S. and Lockington, D.A., (2015). Xylem hydraulic properties in subtropical coniferous trees influence radial patterns of sap flow: implications for whole tree transpiration estimates using sap flow sensors. *Trees*, *29*(4), pp.961-972.

Harris, Huntingford, C, Cox, PM, Gash, JHC & Malhi, Y 2004, Effect of soil moisture on canopy conductance of Amazonian rainforest, *Agricultural and Forest Meteorology*, vol. 122, pp. 215-27. doi:10.1016/j.agrformet.2003.09.006.

Hodgkinson, J., Cox, M. E., McLoughlin, S., & Huftile, G. J. (2008). Lithological heterogeneity in a back-barrier sand island: Implications for modelling hydrogeological frameworks. *Sedimentary Geology*, *203*(1), 64-86. doi:10.1016/j.sedgeo.2007.11.001.

Isaacs and Walker, 1983. Groundwater model for an Island Aquifer: Bribie Island Groundwater study. Department of Civil Engineering, The University of Queensland, St. Lucia.

Jarvis, P. G. (1976). The interpretation of the variations in leaf water potential and stomatal conductance found in canopies in the field. *Philosophical Transactions of the Royal Society of London B: Biological Sciences*, *273*(927), 593-610. DOI: 10.1098/rstb.1976.0035

Jasechko, S, Sharp, ZD, Gibson, JJ, Birks, SJ, Yi, Y & Fawcett, PJ 2013, Terrestrial water fluxes dominated by transpiration, *Nature*, vol. 496, pp. 347-50. doi:10.1038/nature11983.

Jiang, J., DeAngelis, D. L., Teh, S. Y., Krauss, K. W., Wang, H., Li, H., ... & Koh, H. L. (2015). Defining the next generation modeling of coastal ecotone dynamics in response to global change. *Ecological Modelling*. doi:10.1016/j.ecolmodel.2015.04.013.

Kang, Shaozhong, et al. "Crop coefficient and ratio of transpiration to evapotranspiration of winter wheat and maize in a semi-humid region." *Agricultural water management* 59.3 (2003): 239-254.

Kumar, M., Raghuwanshi, N. S., & Singh, R. (2011). Artificial neural networks approach in evapotranspiration modeling: a review. *Irrigation science*, *29*(1), 11-25.doi: 10.1007/s00271-010-0230-8.

Kreuzwieser, J., Papadopoulou, E., & Rennenberg, H. (2004). Interaction of flooding with carbon metabolism of forest trees. *Plant Biology*, *6*(3), 299-306.

Liu, X., Kang, S., & Li, F. (2009). Simulation of artificial neural network model for trunk sap flow of Pyrus pyrifolia and its comparison with multiple-linear regression. *Agricultural water management*, *96*(6), 939-945. doi:10.1016/j.agwat.2009.01.003

Mebane, W.R. & Sekhon, J.S. 2011. Genetic Optimization Using Derivatives: The rgenoud Package for R. Journal of Statistical Software, vol. 42, pp. 1-26.

Monteith, J. L. (1965). Evaporation and environment. In *Symp. Soc. Exp. Biol* (Vol. 19, No. 205-23, p. 4).

Novick, K.A., Oren, R., Stoy, P.C., Siqueira, M.B.S. and Katul, G.G., 2009. Nocturnal evapotranspiration in eddy-covariance records from three co-located ecosystems in the Southeastern US: implications for annual fluxes. *Agricultural and Forest Meteorology*, *149*(9), pp.1491-1504.

Oren, R., Ewers, B.E., Todd, P., Phillips, N. and Katul, G., 1998. Water balance delineates the soil layer in which moisture affects canopy conductance. *Ecological Applications*, *8*(4), pp.990-1002.

Penman, H.L., 1948. Natural evaporation from open water, bare soil and grass. Proceedings of the Royal Society of London A 193, 120–145.

Pfautsch, S, Aspinwall, M, Drake, J, Choat, B, Tissue, D, Burykin, T & Tjoelker, M 2013, 'Putting the puzzle togerther: Investigating hydraulic functioning and water transport at high resolution in tall tress', *9th International Workshop on Sap Flow*, vol. 997.

Schlesinger, W. H., & Jasechko, S. (2014). Transpiration in the global water cycle. *Agricultural and Forest Meteorology*, *189*, 115-117. doi:10.1016/j.agrformet.2014.01.011.

Shuttleworth, W.J., 1993. Evaporation. In: Maidment, D.R. (Ed.), Handbook of Hydrology. McGraw-Hill, Sydney.

Sommer, R., de Abreu Sá, T. D., Vielhauer, K., de Araújo, A. C., Fölster, H., & Vlek, P. L. (2002). Transpiration and canopy conductance of secondary vegetation in the eastern Amazon. *Agricultural and Forest Meteorology*, *112*(2), 103-121. doi:10.1016/S0168-1923(02)00044-8.

25

Stewart, J. B. (1988). Modelling surface conductance of pine forest. *Agricultural and Forest meteorology*, *43*(1), 19-35. doi:10.1016/0168-1923(88)90003-2

van Dam, JC, Huygen, J, Wesseling, JG, Feddes, RA, Kabat, P, Walsum, PEV, Groenendijk, P & Diepen, CA 1997, *Theory of SWAP version 2.0; simulation of water flow, solute transport and plant growth in the soil-water-atmosphere-plant environment*, Wageningen Agricultural University, Dept. of Water Resources, Wageningen.

Wallace, J & McJannet, D 2010, Processes controlling transpiration in the rainforests of north Queensland, Australia, *Journal of Hydrology*, vol. 384, pp. 107-17. doi:10.1016/j.jhydrol.2010.01.015.

Western, AW, Duncan, JM, Olszak, C, Thompson, J, Anderson, T, Grayson, RB, Wilson, D & Young, R 2002, *Calibration of CS615 and TDR instruments for Marhurangi, Tarrawarra and Point Nepean soils*.

Whitley, R, Zeppel, M, Armstrong, N, Macinnis-Ng, C, Yunusa, I & Eamus, D 2008, A modified Jarvis-Stewart model for predicting stand scale transpiration of an Australian native forest, *Plant Soil*, vol. 305, pp. 35-47. DOI: 10.1007/s11104-007-9399-x

Whitley, R, Medlyn, B, Zeppel, M, Macinnis-Ng, C & Eamus, D 2009, Comparing the Penman-Monteith equation and a modified Jarvis-Stewart model with an artificial neural network to estimate stand-scale transpiration and canopy conductance, *Journal of Hydrology*, vol. 373, pp. 256-66. doi:10.1016/j.jhydrol.2009.04.036.

Whitley, R, Taylor, D, Macinnis-Ng, C, Zeppel, M, Yunusa, I, O'Grady, A, Froend, R, Medlyn, B & Eamus, D 2013, Developing an empirical model of canopy water flux describing the common response of transpiration to solar radiation and vapour pressure deficit a five contrasting woodlands and forests, *Hydrological Processes*, vol. 27, pp. 1133-46. DOI: 10.1002/hyp.9280.

Yang, Y., Guan, H., Hutson, J. L., Wang, H., Ewenz, C., Shang, S., & Simmons, C. T. (2013). Examination and parameterization of the root water uptake model from stem water potential and sap flow measurements. *Hydrological Processes*, *27* (20), 2857-2863. DOI: 10.1002/hyp.9406.

Zeppel, M, Tissue, D, Taylor, D, Macinnis-Ng, C & Eamus, D 2010, Rates of nocturnal transpiration in two temperate woodland species with differing water-use strategies, *Tree Physiology*, vol. 30, pp. 988-1000. doi: 10.1093/treephys/tpq053.

Zhang, H, Simmonds, LP, Morison, JIL, Payne, D & Wullschleger, SD 1997, Estimation of transpiration by single trees: Comparison of sapflow measurements with a combination equation, *Agricultural and Forest Meteorology*, vol. 87, no. 155-169. doi:10.1016/S0168-1923(97)00017-8.

1   Tables

2   Table 1: Summary of relevant studies performing transpiration or canopy conductance modelling based on empirical approaches.

3

Study	Model used	Input data	Target data	Location	Vegetation type, tree density	Key results	Soil-water content characterization
Stewart (1988)	Jarvis-Stewart	R_s, D_0, T, SWC	g_c (derived from BREB)	Thetford Forest, UK	*Pinus Sylvestris* (L.) and *Pinus nigra var. maritima* (Ait.), 619 trees ha^{-1}	Non-linear functions including SWC are best to predict g_c.	SWC recorded every few days using a Neutron probe at 0.2, 0.35, 0.5, 0.8 and 1.1 m and integrated over the profile.
Granier and Loustau (1994)	Jarvis-type	R_s, D_0, SWC	g_c (derived from SF)	Landes, Southwest	*Pinus pinaster* (Ait.) of different ages and densities	Inclusion of SWC function in Jarvis-type model.	SWC measured using a Neutron probe at 10 days

				France	(see Granier and Loustau (1994) for details)	Importance of accurate determination of SWC and stand leaf area.	intervals
Sommer et al. (2002)	MLR, Jarvis-type	R_n, T, VPD, D_0	g_c (derived from BREB)	Eastern Amazon, Brazil	Fallow vegetation; Biomass of 22.2 t DM ha^{-1}	MLR outperforms Jarvis-Type models. SWC has to be included in further Jarvis-Type studies.	No SWC included in the modelling.
Harris et al. (2004)	Jarvis-Type	R_n, T, D, SWC	g_c (derived from EC)	Manaus, Brazil	Amazonian rainforest, Biomass 300–350 t ha^{-1}	Inclusion of a SWC function in Jarvis-type model improved the g_c predictions	SWC measured weekly over the top 3.8 m.

Whitley et al. (2008, 2009)	MJS (+ PM and ANN for Whitley et al. (2009))	R_n, VPD, SWC, LAI	T (derived from SF)	Northwestern NSW, Australia	*Eucalyptus crebra* (42 trees ha^{-1}) and *Callitris glaucophylla* (212 trees ha^{-1}) (see Zeppel and Eamus (2008) for details)	MJS performs better than PM for low SWC.	SWC measured at 50 cm depth below surface
Liu et al. (2009)	ANN, MLR	VPD, R_n, T, u, SWC, LAI	T (derived from SF)	Wuwei, Gansu Province, China	Plantation of *Pyrus pyrifolia cv. Pingguoli* (500 trees ha^{-1})	ANN superior to MLR for predicting SF. SWC a key variable for the performance of the ANN.	SWC measured at 5-10 days intervals and integrated over 1 m.
Garcia-Santos et al. (2009)	Jarvis-Stewart	R_s, D_0, T, SWC	g_c (derived from SF)	Canary Island, Spain	*M. Faya* (57%), *E. arborea* (33%), *L. azorica* (10%)	SWC had little influence on g_c even during dry	SWC recorded at 15-min intervals at 0.15 and 0.3 m

30

					1266 trees ha^{-1}	periods. Authors hypothesise deep rooting systems.	below surface and averaged.
Whitley et al. (2013)	MJS, ANN	R_n, VPD, SWC, LAI	T (derived from SF)	Five Australian ecosystems	See Whitley et al. (2013) for details	Site specific versus combined site model calibration shows that combined site calibration works well. SWC function optimisation remains site-specific.	SWC function defined based on permanent and wilting point (according to soil type)

4   MJS: Modified Jarvis Stewart, ANN: Artificial Neural Network, PM: Penman-Monteith, MLR: Multiple Linear Regression, GLM: General Linear Model; SF: Sapflow; BREB:

5   Bowen Ratio energy balance; EC: Eddy covariance.

6   E_0, potential evapotranspiration; RH, Relative Humidity; R_s: Solar radiation; R_n: Net radiation, T: Air temperature; u: wind speed at 2 m; D_0: Specific humidity; g_c: Canopy

7   conductance; LAI: Leaf Area Index.

Table 2: Estimated parameter values and associated standard error from the optimisation of the modified Jarvis Stewart model. The optimization was completed on an ensemble data set of 3 x 20 days with different environmental conditions. Parameters shown are maximum transpiration ($T_{MJS\ max}$), calibration fitted parameters for functional discriptions of net radiation (k_r), vapour pressure deficit (k_{d1}, k_{d2} and D_{max}) and soil moisture (k_s and SWC_w).

Parameter	SC20	SC40	SC60	SC80	SC-Int.
$T_{MJS\ max}$	0.38 (0.02)	0.39 (0.03)	0.38 (0.03)	0.70 (0.19)	0.39 (0.03)
k_r	9.87 (0.30)	9.20 (0.33)	9.89 (0.29)	14.81 (0.24)	8.83 (0.34)
k_{d1}	0.39 (0.33)	0.29 (0.43)	0.38 (0.33)	0.30 (0.38)	0.29 (0.42)
k_{d2}	0.24 (0.46)	0.19 (0.57)	0.24 (0.46)	0.30 (0.35)	0.19 (0.57)
D_{max}	1.70(0.08)	1.86 (0.12)	1.71 (0.08)	1.77 (0.10)	1.86 (0.12)
k_s	354.87 (0.25)	75.60 (0.53)	28.75 (0.34)	15.86 (0.11)	33.58 (0.17)
SWC_w	0.02 (0.02)	0.03 (0.33)	0.07 (0.25)	0.26 (0.09)	0.08 (0.08)

Table 3: Root mean square error (RMSE), coefficient of determination (R^2), slope (m) and intercept (c) of the linear regressions of T_{STAND} versus T_{MJS} (y = mx + c). Observed (T_{STAND}) and predicted (T_{MJS}) cumulative

transpiration fluxes for the full period excluding night-time, cumulative bias, number of days and data points for the calibration and validation periods based on hourly observations and predictions. .

	Scenario	SC20	SC40	SC60	SC80	SC-Int.
Calibration	RMSE (mm)	0.035	0.037	0.035	0.037	0.037
	R^2 (-)	0.93	0.92	0.93	0.92	0.92
	Slope (-)	1.01	1.01	1.00	1.02	1.01
	Intercept (mm)	-0.0025	-0.004	-0.0025	-0.0055	-0.0034
	Cumulative T_{MJS} (mm)	170	156	154	164	158
	Cumulative T_{OBS} (mm)	178	178	178	178	178
	Mean Bias error (mm)	8.0	22	24	14	20
	Nb. days (-)	60	60	60	60	60
	Nb. data points (-)	720	720	720	720	720
Validation	RMSE (mm)	0.049	0.040	0.036	0.041	0.064
	R^2 (-)	0.84	0.89	0.92	0.91	0.85
	Slope (-)	0.95	0.97	1.02	1.02	0.97
	Intercept (mm)	0.002	0.0022	0.0018	-0.0116	0.0245
	Cumulative T_{MJS} (mm)	668	652	567	557	520
	Cumulative T_{OBS} (mm)	643	643	584	535	535
	Mean Bias error (mm)	25	11	17	22	-15
	Nb. days (-)	264	264	243	194	194
	Nb. of data points (-)	3165	3165	2917	2323	2323

List of Figures

Figure 1. (a) and (b) Location of the study site on the east coast of Australia, and (c) location of the main instruments within the experimental plot.

Figure 2. Daily time averages of: (a) rainfall, (b) net radiation (R_n), (c) vapour pressure deficit (VPD), (d) observed sapflow-based transpiration (T_{STAND}), (e) soil-water content (SWC) and (f) water table elevation relative to surface. Lines on (b) and (c) are 10 days moving averages and vertical bars on (d) are standard deviations on T_{STAND} as explained in the text.

Figure 3. Functional dependencies from the fitted parameters of Hourly T_{MJS} on (a) hourly R_n and (b) hourly VPD for SC20. The left y-axis represents data points and the right y-axis the normalized fit of the functions (T_{MJS} / $T_{MJS\,max}$). The data points are separated into four seasons (summer of 2012 (01/01/2012 to 29/02/2012), autumn 2012 (01/03/2012 to 31/05/2012), winter 2012 (01/06/2012 to 31/08/2012), spring of 2012 (01/09/2012 to 30/11/2012) and summer of 2013 (01/12/2012 to 31/01/2013).

Figure 4. Water table elevation relative to surface *versus* ratio of observed transpiration (T_{STAND}) over potential evapotranspiration.
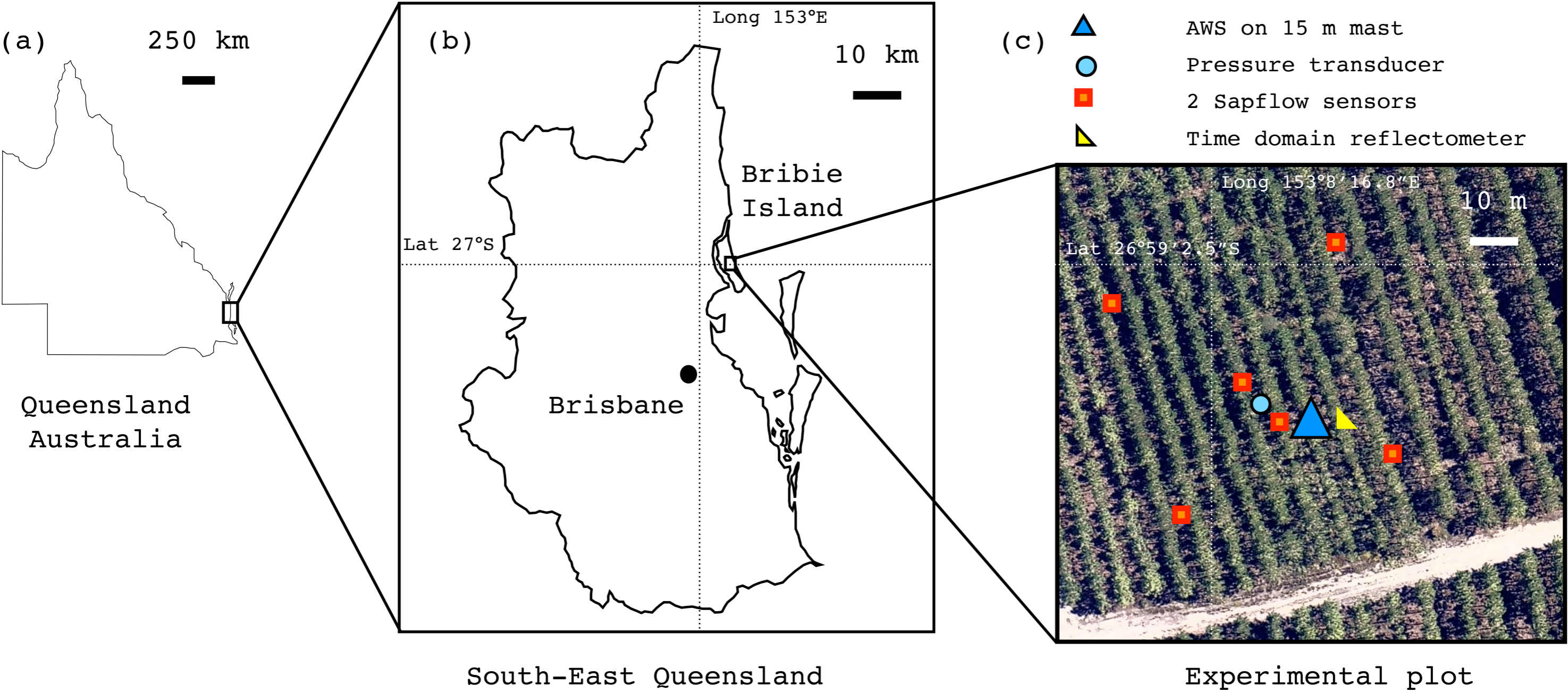
Figure 5. Soil-water content function from the fitted parameters of stand transpiration: (a) SC20, (b) SC40, (c) SC60, (d) SC80 and (e) SC-Int. The left y-axis represents data points and the right y-axis the normalized fit of the soil functions (T_{MJS} / $T_{MJS\,max}$). The data points are separated into summer, autumn, winter and spring using the same periods as defined for Figure 3.
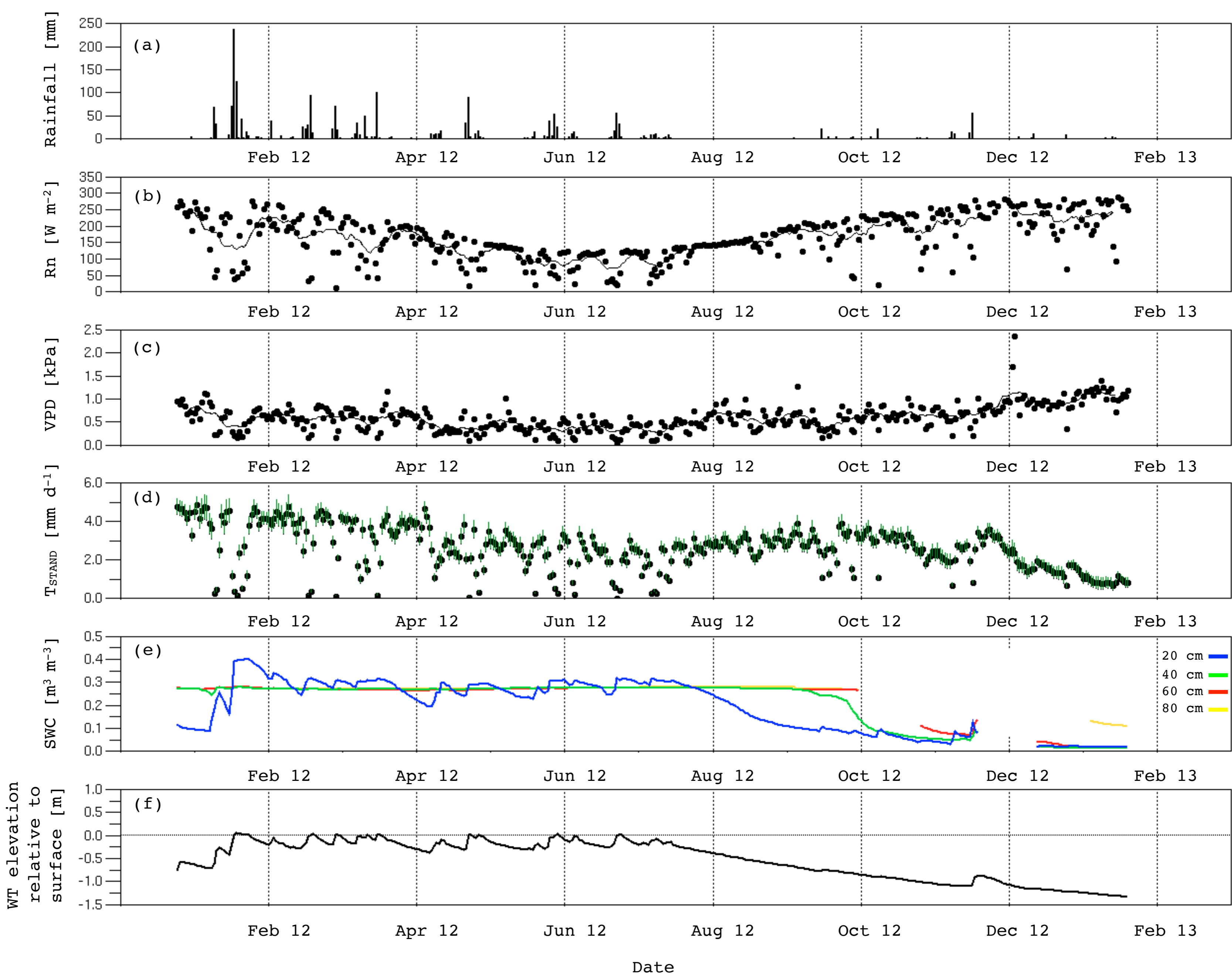
Figure 6. Observed (T_{STAND}) versus predicted (T_{MJS}) hourly transpiration fluxes as well as linear regressions for the validation period for (a) SC20, (b) SC40, (c) SC60, (d) SC80 and (e) SC-Int.
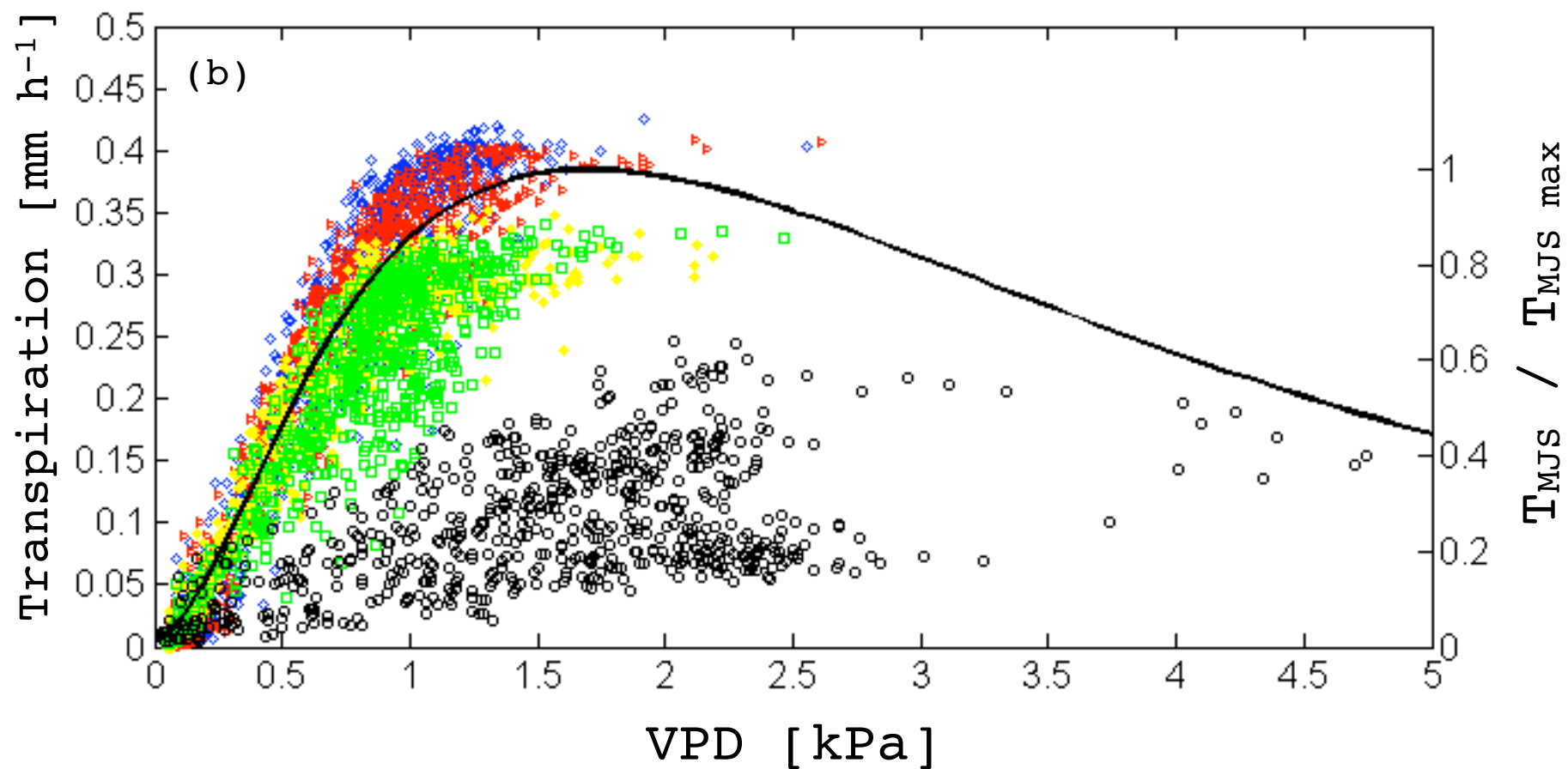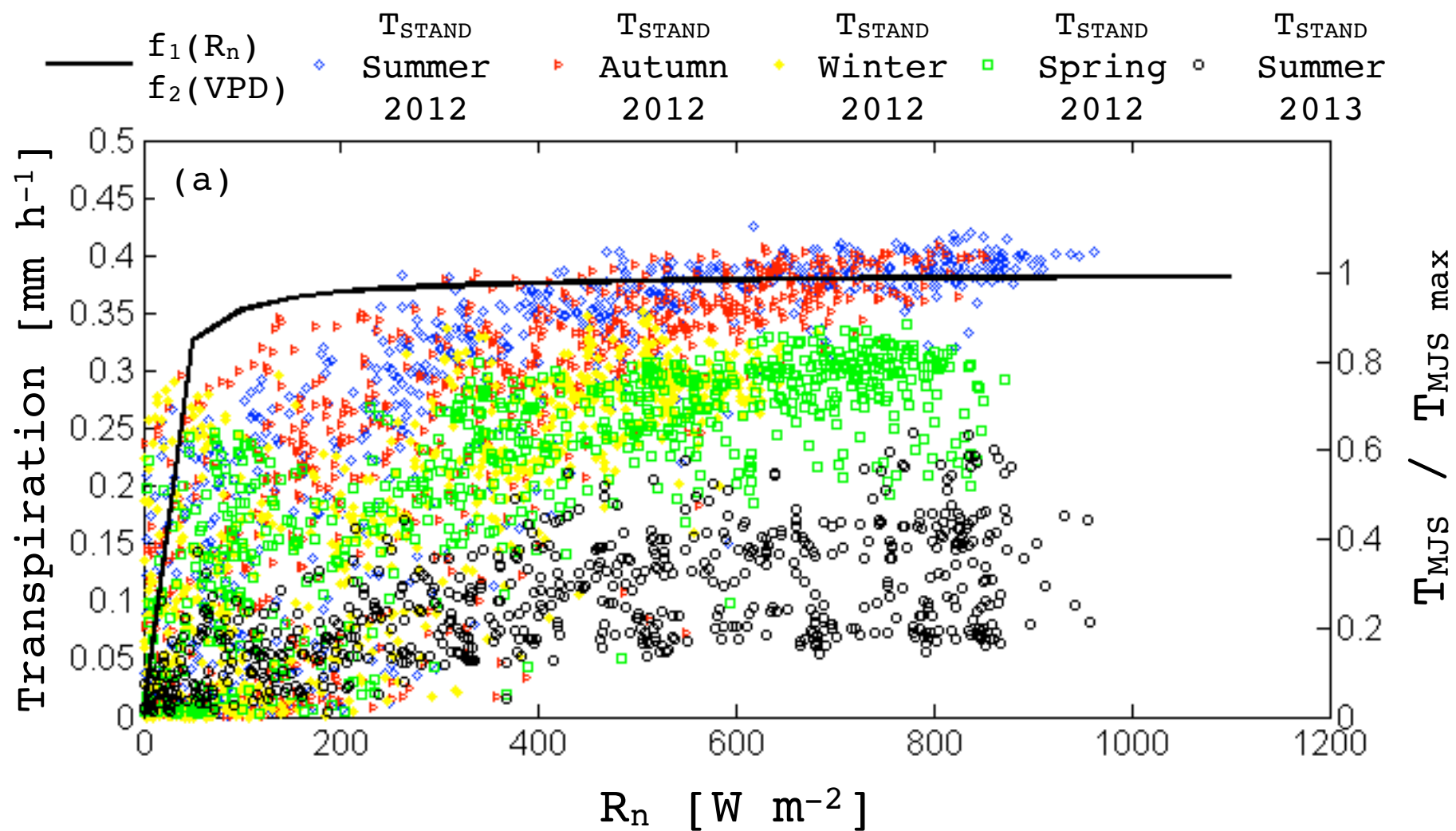
Highlights

. We tested a *Modified Jarvis-Stewart* model for a subtropical shallow aquifer forest.

. Transpiration is water-unlimited for a water table above a threshold depth of 0.8m.

. Transpiration decreases linearly with increasing water table depth below 0.8m.

. Wet season modelled-transpiration is independent from soil moisture characterisation.

. Dry season modelled-transpiration is dependent on the soil moisture characterisation.

(a) Queensland Australia — 250 km

(b) South-East Queensland — Long 153°E, Lat 27°S, Bribie Island, Brisbane, 10 km

(c) Experimental plot — Long 153°8′16.8″E, Lat 26°59′2.5″S, 10 m

AWS on 15 m mast
Pressure transducer
2 Sapflow sensors
Time domain reflectometer

Figure 6

(a) $y = 0.9516x + 0.002$ $R^2 = 0.83708$ SC20

(b) $y = 0.9745x + 0.0022$ $R^2 = 0.88764$ SC40

(c) $y = 1.0226x + 0.0018$ $R^2 = 0.91511$ SC60

(d) $y = 1.0152x - 0.0116$ $R^2 = 0.91053$ SC80

(e) $y = 0.9655x + 0.0245$ $R^2 = 0.85416$ SC-Int.

T_{MJS} [mm h^{-1}] T_{STAND} [mm h^{-1}]